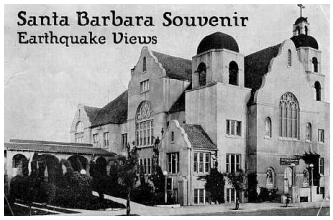

4th IASPEI / IAEE International Symposium:

Effects of Surface Geology on Seismic Motion

August 23–26, 2011 · University of California Santa Barbara

EFFECTS OF EXISTING LANDSLIDES ON SEISMICALLY-INDUCED DISPLACEMENTS DUE TO INPUT-SLOPE INTERACTIONS

Luca LENTI
IFSTTAR
Paris East University
France

Salvatore MARTINO
CERI- Dip. Scienze della Terra
University of Rome "Sapienza"
Italy

ABSTRACT

Preliminary results of a numerical study on input-slope interaction for evaluating the co-seismic displacements of existing landslides are here presented. Three slope geometries with a dip varying in the range 10°-45° are considered; 53 multifrequential dynamic equivalent signals were applied to the models and were derived according to the LEMA_DES approach from the accelerometric records of the European Strong Motion and of the COSMOS databases. These signals are characterised by Arias intensities in the range 0.001-10 m/s and by PGAs in the range 0.1-1 m/s^2. The simulations performed until now are referred to linear conditions and to sliding landslide mechanisms. The results point out that lower is the dip of the slope higher are the induced displacements; a parametric analysis on the mechanical properties as well as on the characteristic period of the seismic inputs proved that the displacement values depend on the 2D seismic amplification of the landslide mass. The seismically-induced displacements obtained by dynamic analysis can be significantly differ from the ones computed by sliding block methods, also depending on the critical pseudostatic threshold of the landslide.

INTRODUCTION

Seismically-induced slope instabilities are often responsible for the greatest damages and losses due to earthquakes (Bird and Bommer, 2004); empirical correlations have been proposed (Keefer, 1984; Rodriguez et al. 1999) between the epicentral distance of the landslides and the magnitude of the triggering earthquakes. Nevertheless, these correlations may be altered by local site conditions (tectonic features, stratigraphic conditions, morphology), which modify the seismic motion. The possible interactions between seismic waves and slopes for predicting seismically-induced landslide movements were recently analysed (Martino and Scarascia Mugnozza, 2005; Sepulveda et al., 2005; Del Gaudio and Wasowsky, 2007; Bozzano et al., 2008b; Danneels et al., 2008; Bozzano et al., 2011) in order to point out how both landslide mechanisms and triggering conditions depend on seismic input properties such as energy, frequency content, directivity and peak of ground acceleration (PGA). In particular, some case studies pointed out the role of "self-excitation" process (Bozzano et al., 2008b), due to seismic amplification effects, in triggering far field pre-existing large landslide, which represent outliers with respect to the predictive curves proposed by Rodriguez et al., 1999.
The effects of seismic amplification due to specific topographies, such as ridge and canyon, were studied since the 1970s by different Authors (Sanchez-Sesma and Rosenblueth, 1979; Geli et al., 1988; Athanasopoulos et al., 1999; Zaslavsky and Shapira, 2000; Bakavoli and Hagshenhas, 2010), on the basis of instrumental data from strong earthquake which suggested that surface topography contributes to modify the seismic ground motion. Nevertheless, the effects of step-like slope topography on seismic ground motion was only recently studied by some Authors (Ashford et al., 1997; Bouckovalas and Papadimitriou, 2005; Nguyen and Gatmiri, 2007, Papadimitriou and Chaloulos, 2010) via numerical modeling, since results from field measurements are difficult to obtain due to the wave scattering that the step-like slope geometry produces.
The interaction of seismic waves with slope can also influence the permanent induced deformations in the case of both unsheared slopes, which were not yet affected by landslide processes, and of sheared slopes, i.e. with pre-existing landslide masses.
In this regard it's worth noting that, for a given acceleration time history, the expected co-seismic displacements within slopes are commonly evaluated by applying Newmark's sliding block method (Newmark, 1965). More recently, the sliding block displacement methodology was improved to account for coupled interaction between sliding and dynamic responses by an analytical procedure to

simultaneously estimate the seismically-induced permanent displacements due to stick-slip events of sliding and the 1D deformable dynamic response of the structure that exhibits a significantly nonlinear behaviour (Rathje and Bray, 2000; Rathje and Antonakos, 2010). In these latter studies, the coupled analyses indicates that the accelerations within the sliding mass often exceed the yield acceleration at its base, due to the dynamic response of the sliding mass.
Nevertheless, the ultimate-limit-state criterion at the basis of the Newmark's method does not allow to take into account the interaction between slopes and seismic inputs in terms of local amplification/de-amplification of the ground motion due to both topography of the slope and geological setting. On the contrary, stress-strain numerical analysis, performed under dynamic conditions, can contribute to this topic and quantify the expected strain effects due to seismic shaking.
In this regard, the here proposed numerical study is focused on the interaction between seismic inputs and sheared slopes, which host pre-existing landslide masses, in order to evaluate the possible role of seismic amplification in seismically-induced landslide movements and to quantify the induced displacements.

PERFORMED NUMERICAL MODELING OF SHEARED SLOPES

In order to evaluate the seismic amplification effects due to slopes in terms of both geometry and geological setting, a preliminary numerical modeling was performed on 3 different slope configurations, before applying the different inputs to force them toward landslide processes. The considered soil is a high consistency clay while the geometries of the slope were designed according to a step-like topography (Fig.1).

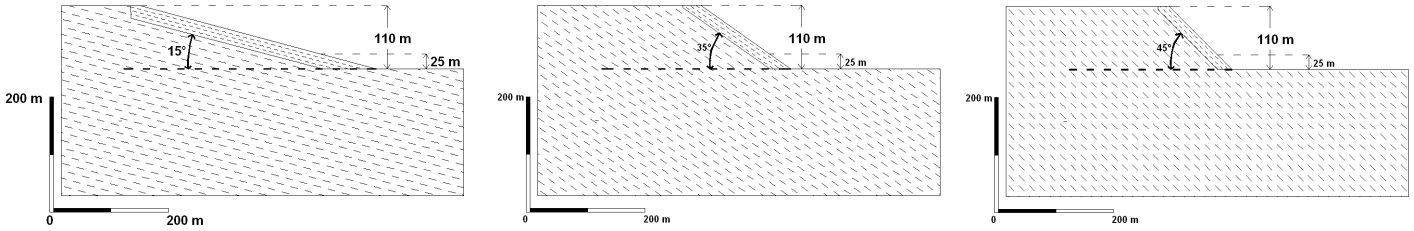

Fig. 1. Considered step-like slope configurations: the denser fill indicates the landslide mass

More in particular, the three slope configurations were designed according to the sketch reported in Fig.1, i.e. by assuming three slope inclinations (15°, 35° and 45°); the slope configurations host pre-existing landslide masses which can be regarded as prone to mainly translational landslides (Cruden and Varnes, 1996).
The selected sliding surfaces correspond to a fundamental period (Rathje and Bray, 2000) T_s equal to 0.25 s, i.e. are characterised by a thickness of 25 m and a shear wave velocity (Vs) equal to 400 m/s. According to an "infinite slope" model the static safety factor (SF_0) of the landslide masses are equal to 1.42, 1.19 and 1.14 for the 15°, 35° and 45° dip configurations respectively, while the critical accelerations (k_y) are equal to 0.1 g. On the other hand, the values of the characteristic period due to the length on the landslide mass (T_l) vary in the range 0.4-0.9 s.

Table 1. Mechanical parameters of the considered soils

	slope dip	constitutive law	den *kg/m³*	ν	G_0 *Pa*	Vs *(m/s)*	ϕ *(°)*	c *Pa*	ten *Pa*	dil *(°)*
clay	all	Mohr-Coulomb	2110	0.25	2.55E+09	1.10E+03	24	1.33E+05	1.30E+04	14
clay (landslide mass)	15°	Mohr-Coulomb	2110	0.25	3.38E+08	4.00E+02	16	4.60E+04	1.60E+05	14
clay (landslide mass)	35°	Mohr-Coulomb	2110	0.25	3.38E+08	4.00E+02	18	1.80E+05	5.54E+05	14
clay (landslide mass)	45°	Mohr-Coulomb	2110	0.25	3.38E+08	4.00E+02	19	2.10E+05	6.10E+05	14

Physical and mechanical parameters of the considered soils are reported in Tab.1 and they are referred to a preliminary approach, i.e. a visco-elastic-perfectly plastic behaviour was assumed. The parameter values attributed to the models are based on laboratory tests performed on undisturbed samples of over-consolidated (OCR≅2) high-consistency clays, which widely outcrop in Southern and Central Italy in correspondence of slopes involved in landslides (Bozzano et al., 2006; Bozzano et al., 2008a). On the other

hand, the adopted stiffness values for landslide debris guarantee a significant impedance contrast (i.e. equal to 3) between the landslide mass and its substratum. Nevertheless, a parametric study was here performed by gradually increasing the stiffness of the landslide mass.

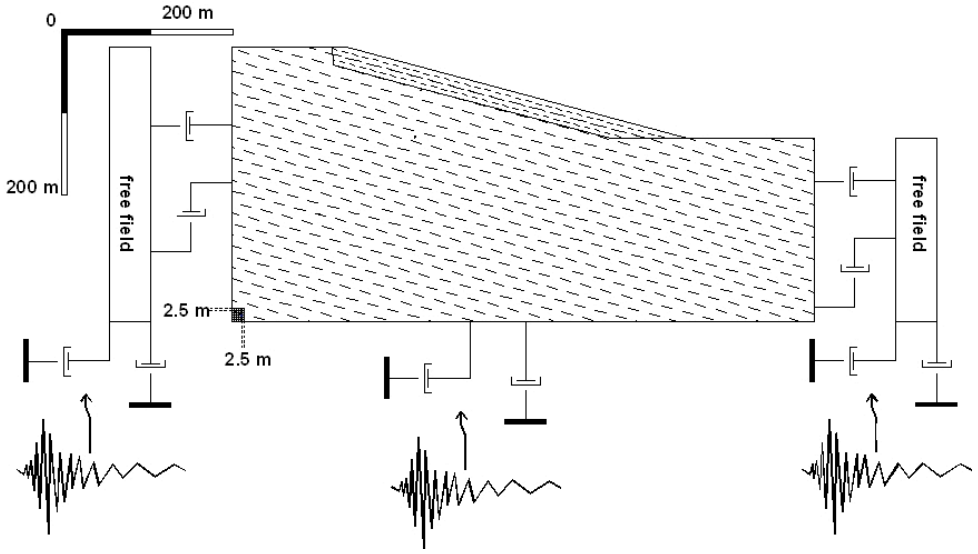

Fig. 2. Schematic illustration of the 2D numerical models, including mesh resolution and boundary conditions (see Fig.1 for legend).

Energy dissipation was computed using a Rayleigh Damping function equivalent to generalized Maxwell model (Zienkiewicz 2005; Semblat and Pecker, 2009); the assumed damping function guarantees that at each shear strain level the maximum damping coefficient varies from 0.05 up to 0.5 within the whole frequency range 0-10Hz. Moreover, the adopted 2.5 m square grid is consistent with the frequency range of interest (i.e. up to 10 Hz). In order to minimize the effects of artificial wave reflections from the boundaries, the total width and the total height of the mesh are greater than the double dimension of the slope while transmitting boundary was applied at the base of the mesh and free field boundaries were applied at the left and right sides.
A schematic illustration of the 2D numerical models, including mesh resolution and boundary conditions is reported in Fig.2.

NUMERICAL MODELING

Amplification functions

In order to evaluate the seismic amplification due to the slope configurations a delta-like Gabor function (*G(t)*), was applied in the form of a vertical upward SV stress-wave.
The choice of the Gabor function's parameters ensures a negligible spectral amplitudes of the resulting signal for frequencies higher than 10 Hz. To avoid numerical errors during dynamic calculation, the function has a symmetrical shape and a null integral on the total time.
The numerically-derived seismic amplification functions (A(f)) for the 3 considered slope configurations of Fig.1 are reported in Fig.3 and represent the acceleration spectral ratios between the superficial receivers, located along the slope topographical surface and the outcropping bedrock.
The obtained results show de-amplification effects (A(f) down to 0.6) just along the slopes, in the case of 35° and 45° slope inclination, while amplification effects (A(f) up to 2.5) result all along the slope, i.e. in correspondence to the landslide mass, in the case of 15° slope inclination. In this case the obtained A(f) function shows that the highest amplifications correspond to the resonant frequency of the landslide mass (i.e. 3-4Hz).

Input selection

In order to perform the dynamic numerical analysis, on the three adopted sheared slope configurations, 53 accelerometric records were selected from the European Strong Motion and of the COSMOS databases; the 11 March 2011 waveform recorded on the ground floor of an office building in Sendai (Honshu, Japan) by station B2F of the Building Research Institute, 150 km west of the epicentre was also considered (Lenti et al., 2011). The selected records are characterized (see Tab. 2) by Arias intensities varying in the range 0.001-10 m/s and by PGAs varying in the range 0.1-1 m/s^2; moreover, according to Bray and Rathjie (1998), the values of the characteristic period, T_m, of the records vary in the range 0.09 – 2.17 s and, as a consequence, the values of the characteristic ratio T_s/T_m for the sheared slope geometries vary in the range 0.1 – 2.7.

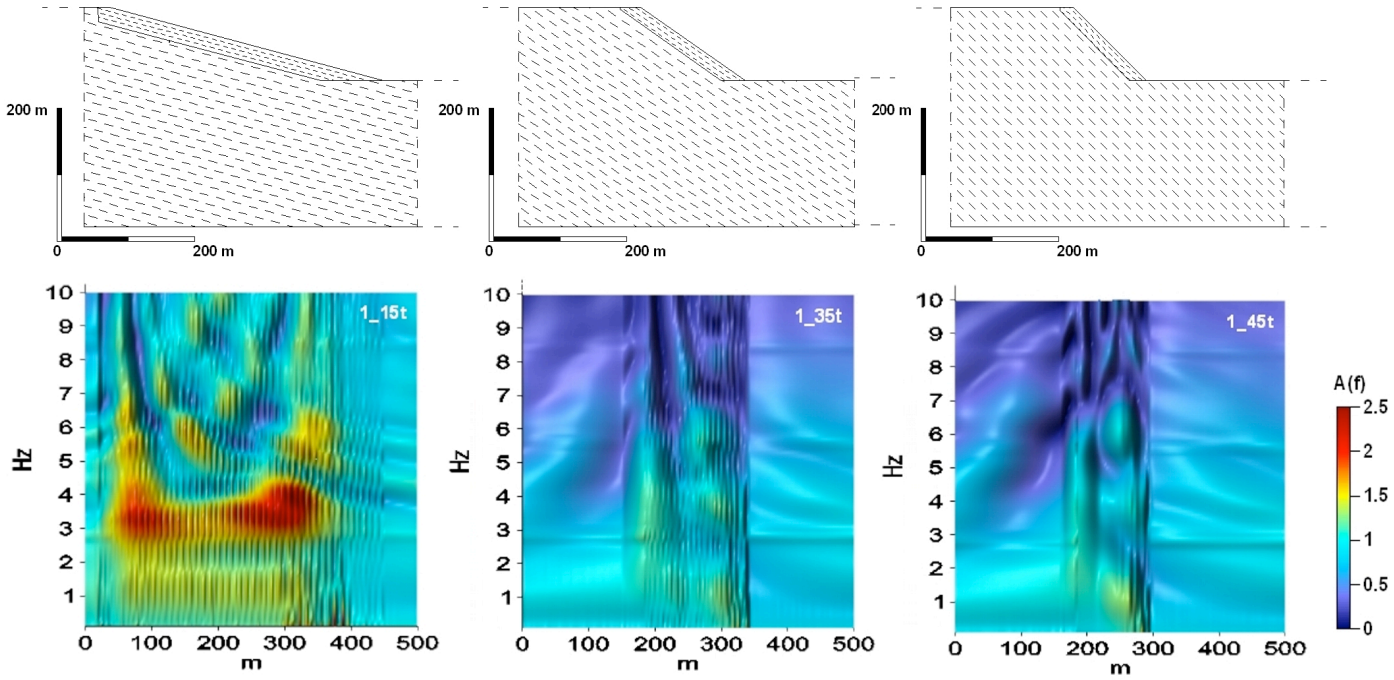

Fig. 3. Amplification functions A(f) obtained for the considered slope configurations.

An equivalent signal was associated to each selected input (Fig.4) according to the LEMA_DES (Levelled-Energy Multifrequencial Analysis for deriving Dynamic Equivalent Signals) approach by Lenti and Martino (2010). The use of the LEMA_DES approach may: i) check that the frequency content of the derived signals is defined within a representative/admissible range; ii) avoid upper-threshold frequency to be exceeded in the modeling; iii) narrow the energy gap between real and simulated seismic actions; iv) control the maximum intensity of the adopted action and v) take into account seismically-induced effects arising from frequency combinations, i.e. from dynamic actions.

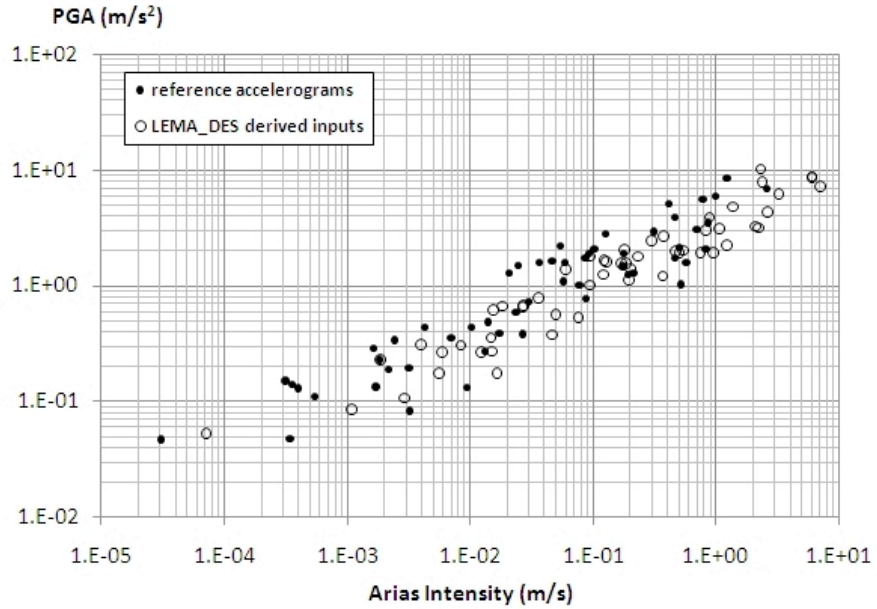

Fig. 4. Arias intensity vs. PGA for the 53 considered natural accelerograms and for the corresponding LEMA_DES derived equivalent signals.

Table 2. Parameters of the natural earthquakes (listed for increasing PGA) and of the LEMA_DES derived equivalent signals (_eq), used for the here performed numerical modeling. Stars (*) indicate the 26 earthquakes selected for the parametric analyses.

Earthquake	Date (yyyymmdd)	Mw	Epicentral distance (km)	Arias (m/s)	PGA (m/s^2)	Arias_eq (m/s)	PGA_eq (m/s^2)
Duzce2 (aftershock)	20000707	4.5	160	7.14E-05	0.05	3.07E-05	0.05
Duzce1	19991112	7.2	177	1.09E-03	0.09	3.43E-04	0.05
Izmit (aftershock)	19990831	5.2	38	1.87E-03	0.23	5.49E-04	0.11
Izmit	19990817	7.6	330	2.91E-03	0.11	3.19E-03	0.08
Friuli (aftershock)*	19760611	4.7	1	3.96E-03	0.31	1.62E-03	0.29
Izmit (aftershock)	19990831	5.2	39	5.56E-03	0.18	1.71E-03	0.14
Umbria Marche (aftershock)*	19971012	5.3	14	5.86E-03	0.27	4.00E-04	0.13
Mt.Hengill Area	19980604	5.5	18	8.42E-03	0.31	2.15E-03	0.19
Lazio Abruzzo (aftershock)	19840511	5.5	15	1.24E-02	0.27	1.82E-03	0.23
Javakheti Highland*	19901216	5.5	70	1.47E-02	0.36	3.15E-04	0.15
Duzce1	19991112	7.2	42	1.51E-02	0.27	3.18E-03	0.20
Izmit (aftershock)*	19991107	5.0	5	1.53E-02	0.62	3.54E-04	0.14
Duzce1	19991112	7.2	185	1.65E-02	0.18	9.38E-03	0.13
Friuli (aftershock)	19760911	5.3	8	1.83E-02	0.67	2.42E-03	0.34
Almiros (aftershock)	19800811	5.3	14	2.68E-02	0.67	7.02E-03	0.36
Kozani (aftershock)*	19950611	4.8	3	2.72E-02	0.68	4.26E-03	0.44
Friuli (aftershock)	19760611	4.7	1	3.60E-02	0.79	1.40E-02	0.49
Bucharest	19770304	7.5	484	4.64E-02	0.38	1.33E-02	0.27
Komilion*	19940225	5.4	16	4.96E-02	0.57	1.03E-02	0.44
Izmit	19990817	7.6	93	7.55E-02	0.54	2.66E-02	0.38
Oelfus	19981113	5.2	11	6.02E-02	1.40	3.61E-02	1.61
Duzce1*	19991112	7.2	11	9.43E-02	1.02	2.36E-02	0.59
Ionian	19731104	5.9	15	1.20E-01	1.26	1.72E-02	0.39
Alkion*	19810224	6.6	20	1.95E-01	1.13	2.99E-02	0.73
Lazio Abruzzo*	19840507	5.9	16	2.02E-01	1.42	5.75E-02	1.10
Manjil	19900620	7.4	131	3.69E-01	1.22	2.13E-01	1.30
Umbria Marche*	19970926	5.7	23	9.44E-02	1.80	2.09E-02	1.29
Umbria Marche (aftershock)*	19980405	4.8	10	1.23E-01	1.67	5.45E-02	2.23
Friuli (aftershock)*	19760911	5.3	21	1.28E-01	1.62	2.46E-02	1.50
Friuli (aftershock)	19760915t	6.1	25	1.71E-01	1.57	4.63E-02	1.64
BassoTirreno	19780415	6.1	18	1.83E-01	1.56	8.80E-02	0.77
Umbria Marche (aftershock)	19971003	5.3	5	2.33E-01	1.80	7.66E-02	1.02
Umbria Marche	19970926b	6.0	5	4.70E-01	1.99	1.94E-01	1.25
Honshu*	20110311	9.0	133	5.00E-01	1.94	4.98E-01	2.14
Bucharest	19770304	7.5	161	7.46E-01	1.95	5.70E-01	1.61
Izmit	19990817	7.6	94	9.52E-01	1.93	5.15E-01	1.03
Dursunbey*	19790718	5.4	6	1.80E-01	2.07	8.65E-02	1.76
Ano Liosia*	19990907	6.0	14	2.97E-01	2.45	5.91E-02	1.61
Montenegro	19790415	7.0	25	5.39E-01	2.02	9.20E-02	1.91
Montenegro	19790415	7.0	24	1.22E+00	2.23	4.64E-01	1.76
Parkfield*	19660627	6.1	15.7	3.74E-01	2.70	1.02E-01	2.07
Hyogoken-Nambu*	19950116	6.9	25.5	8.17E-01	3.05	1.75E-01	1.90
Tabas*	19780916	7.4	20.77	8.80E-01	3.93	1.27E-01	2.81
Northridge*	19940117	6.7	39	1.06E+00	3.10	4.16E-01	5.12
Northridge*	19940117	6.7	36	1.37E+00	4.83	4.59E-01	3.92
Northridge	19940117	6.7	14.9	2.11E+00	3.27	6.96E-01	3.06
Northridge*	19940117	6.7	15.8	2.20E+00	3.19	3.13E-01	2.95
Cape Mendocino	19920425	7.1	10.5	2.31E+00	10.19	1.75E-01	1.48
Duzce1*	19991112	7.2	39	2.38E+00	7.88	8.55E-01	3.52
Loma Prieta*	19891018	6.9	16.3	2.62E+00	4.33	7.78E-01	5.60
Loma Prieta*	19891018	6.9	7	3.24E+00	6.18	9.91E-01	5.94
Superstition Hill*	19871124	6.7	7.5	6.02E+00	8.77	2.57E+00	6.93
Tabas*	19780916	7.4	57	6.03E+00	8.64	1.23E+00	8.45
Landers	19929628	7.3	44	7.02E+00	7.17	8.25E-01	2.10

More in particular, the LEMA_DES procedure generates a sequence of functions and signals which: 1) provides the selection of characteristic frequencies from a smoothed Fourier spectrum of a reference accelerogram; 2) achieves a null integral over the entire duration of the final signal and a spectral density negligible at

frequencies lower than the minimum characteristic one; 3) generates a resulting multifrequencial dynamic equivalent signal, which is energy-equivalent to the reference one, best fitted in terms of PGA via an iterative procedure performed on the number of equivalent cycles and whose time duration is significantly shorter than the reference one.

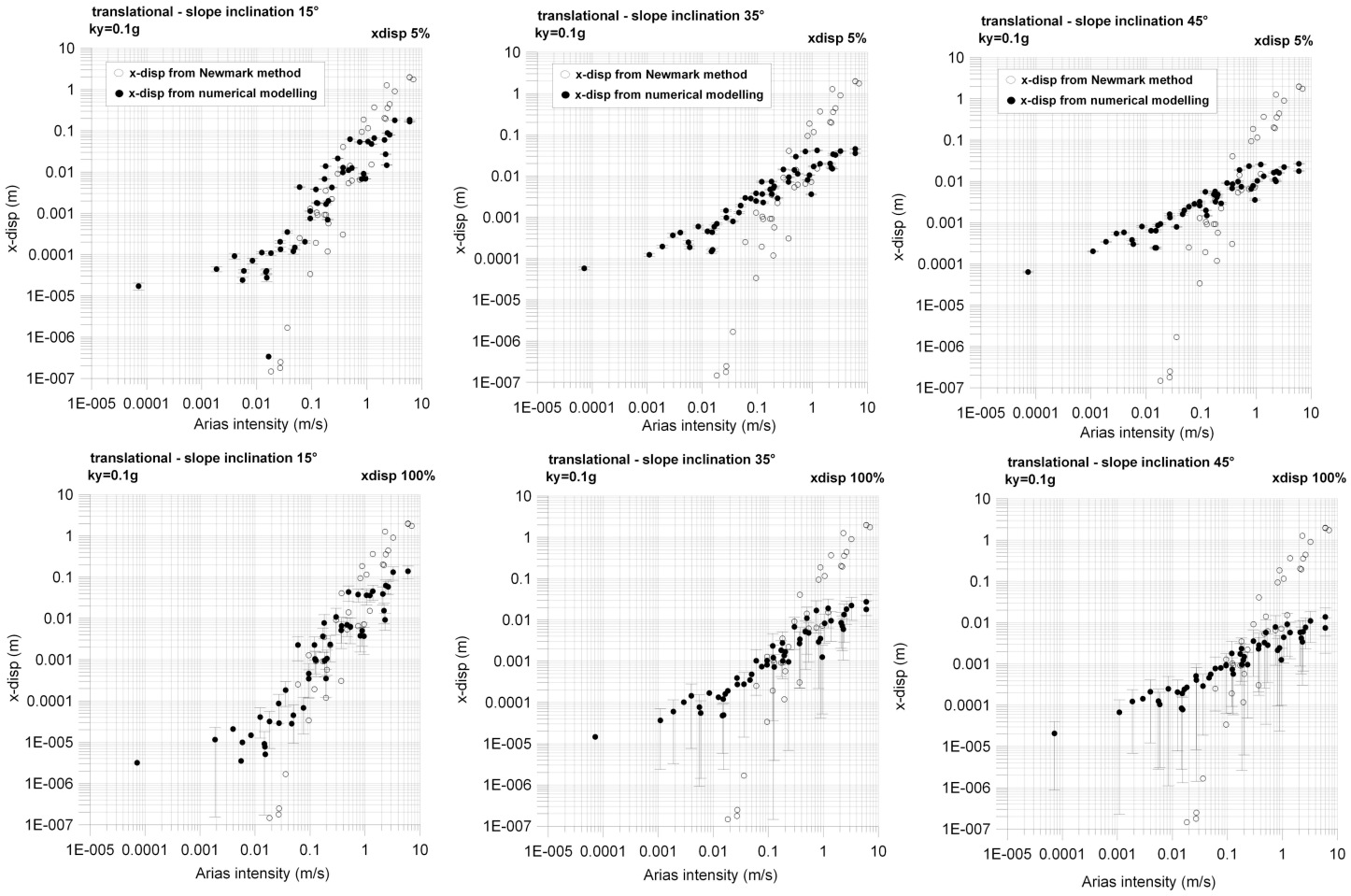

Fig. 5. Arias intensity vs. x-displacements for the 3 considered slope configurations and for the 53 applied earthquakes, resulting from the dynamic numerical modeling and computed by Newmark sliding block analysis. Error bars show the values of standard deviation computed by averaging the x-displacement resulting by the numerical modeling respect to the 5% (upper row) and to the 100% (lower row) of the landslide mass.

Dynamic parametric analysis on the sheared slope configurations

In order to analyse the effects due to the input-slope interaction on the 3 selected slope configurations of Fig.1, all the 53 selected inputs were applied to the models and horizontal displacements (x-displacements) were computed taking into account the mobility of the landslide mass only respect to the substratum.
More in particular, the x-displacements were computed by averaging the values within the landslide which result for different percentages of the whole mass (i.e. obtaining different distributions of x-displacements values at 5%, 15%, 30%, 50% and 100% respect to the total volume for unit depth of the landslide mass).
A selection of 26 inputs (see Tab.2), whose Arias Intensity values are uniformly distributed within the considered range (i.e. 10^{-4} – 10 m/s), was used to force the models in order to evaluating : i) the effect of reduced impedance contrast between the landslide mass and the substratum (i.e. decreasing the impedance contrast from 3.0 down to 1.5), ii) the effect due to different values of the k_y (i.e. 0.1g and 0.5g) referred to the existing landslide. Moreover, the influence on landslide displacements, due to different frequency contents of seismic inputs was analyzed by generating 17 synthetic dynamic multifrequential signals, characterized by T_m values varying in the range 0.1 – 2 s and by Arias intensity values close to 1 m/s.

RESULTS

The results obtained from the parametric numerical modeling performed under dynamic conditions demonstrate that higher is the dip of the slope lower are the expected x-displacements for the same Arias Intensity as well as for the same PGA of the seismic input.
If the expected x-displacements are compared with the ones computed by Newmark sliding block method it is worth noting that for Arias intensity values lower than 0.1 m/s the resulting dynamic x-displacements are mainly underestimated while, on the contrary, they are overestimated for higher Arias intensity values (Fig.5). Nevertheless, overestimation is much more important in the case of slopes characterized by low angle of dip (i.e. <35°). The results demonstrate that, in the case of Arias intensity values of the seismic input lower than 0.1 m/s, higher are the percentages of x-displacements average values respect to the whole landslide mass (i.e. from 5% up to 100%) more relevant are the related values of standard deviation.
Moreover, for a higher k_y value (i.e. 0.5g) x-displacements show a lower dependence on the dip of the slope but their values are generally higher than the ones computed by Newmark sliding block method, within the whole considered range of Arias intensity values (Fig.6). On the contrary, by reducing the impedance contrast between the landslide mass and the substratum, the x-displacements resulting by the numerical modeling gradually underestimate the ones computed according to the Newmark approach (Fig.7).

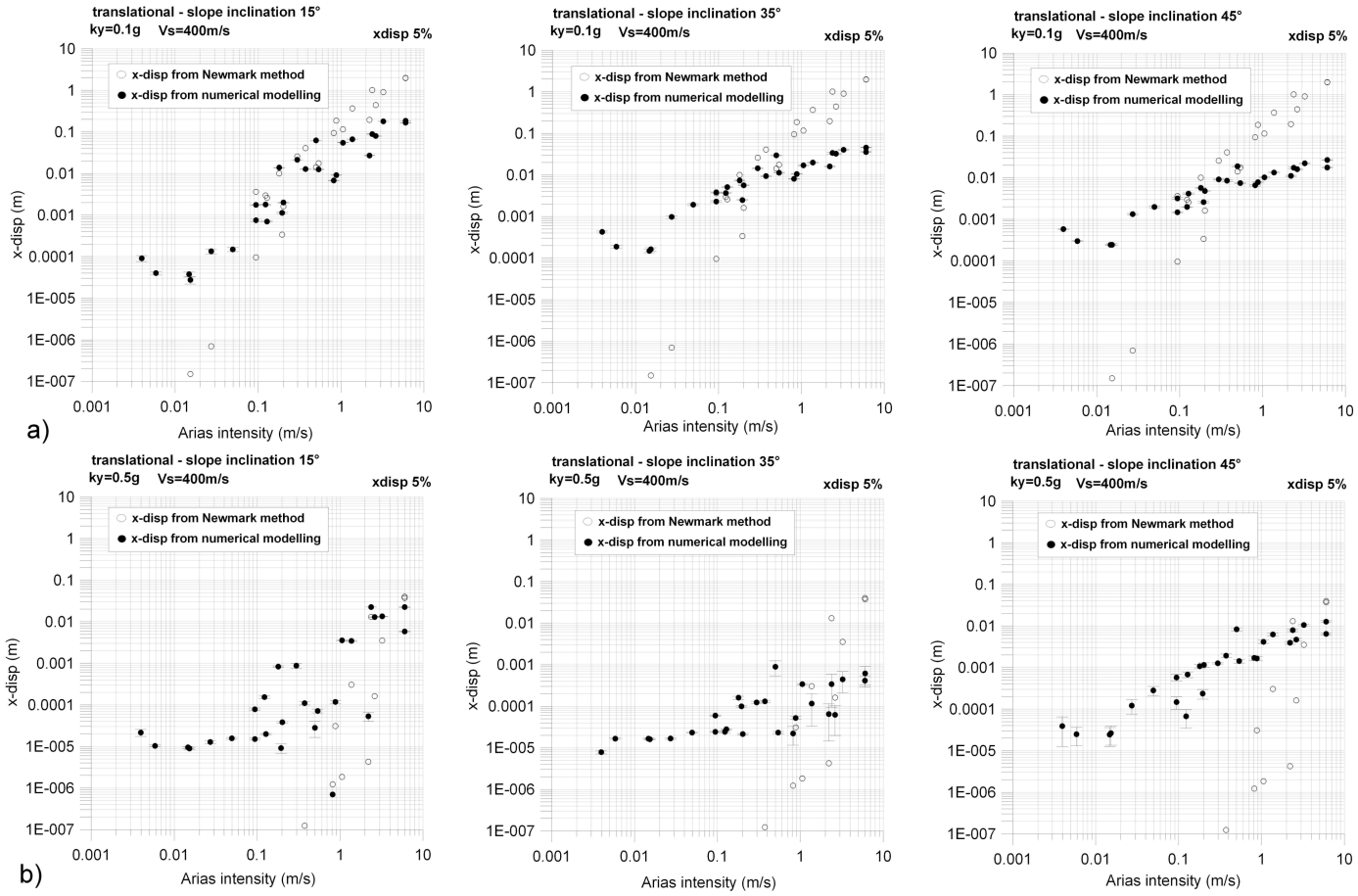

Fig. 6. Arias intensity vs. x-displacements (for the three slope configurations and for the 26 selected earthquake) as they result by varying k_y from 0.1g (a) up to 0.5g (b).

In order to analyze the effects of the seismic input frequency content on landslide displacements the ratios T_s/T_m and T_l/T_m were considered vs. the x-displacements derived from the dynamic numerical modeling. At this aim, 17 synthetic dynamic multifrequential signals, characterized by an Arias intensity close to 1 m/s, were applied to the models; the results highlight that the modelled x-displacements generally show a relevant decrease with increasing dip of the slope; moreover, no relevant correlations exist in the case of T_s/T_m ratio since at the characteristic landslide mass resonant frequency (i.e. at T_s/T_m ratio equal to 1, with reference to a only 1D

local seismic amplification) it does not correspond the maximum x-displacement value (Fig.8a). In this regard, it is worth noting that these results do not fit the ones obtained by Rathjie and Bray (2000) by the application of a flexible sliding block approach which only takes into account the 1D amplification due to the resonance of the landslide mass.
On the other hand, the T_l/T_m values vs. the x-displacements derived from the numerical modeling (i.e. with reference to a 2D input-slope interaction) show a good correlation, since at the halved values of the characteristic length period (T_l) of the landslide (i.e. T_l/T_m equal to about 0.5) correspond the maximum values of the x-displacements (Fig.8b); nevertheless, it is worth noting that the maximum peak occurs at values of the T_l/T_m ratio which decrease with increasing dip of the slope.

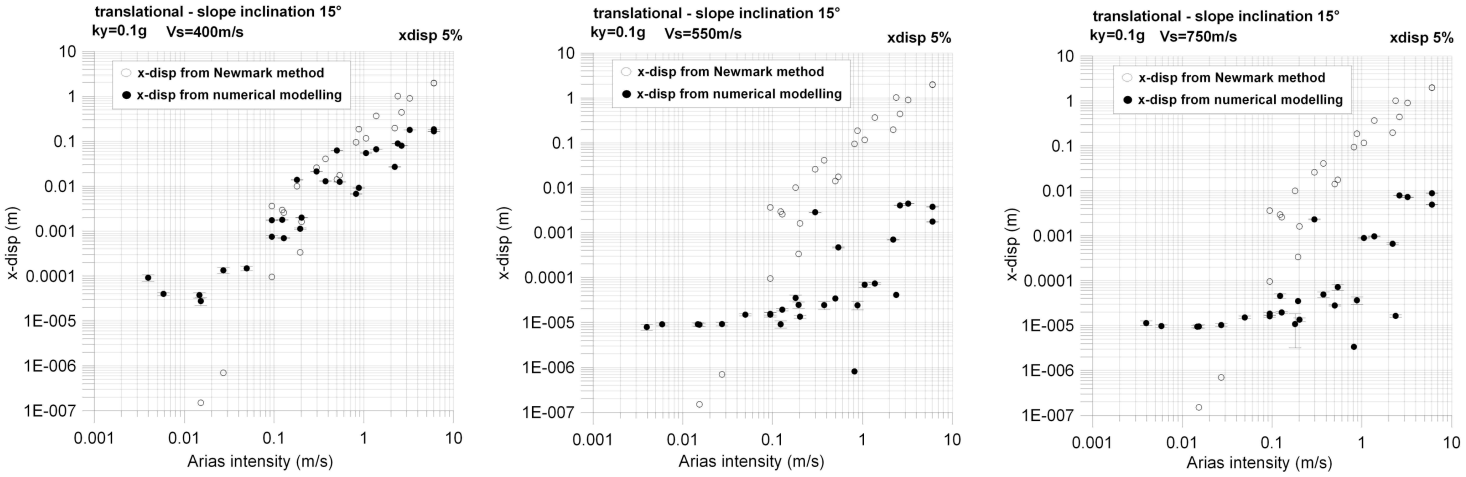

Fig. 7. Arias intensity vs. x-displacements (for the 15° slope configurations and for the 26 selected earthquake) as they result by varying Vs impedance contrast between the landslide mass and the substratum .

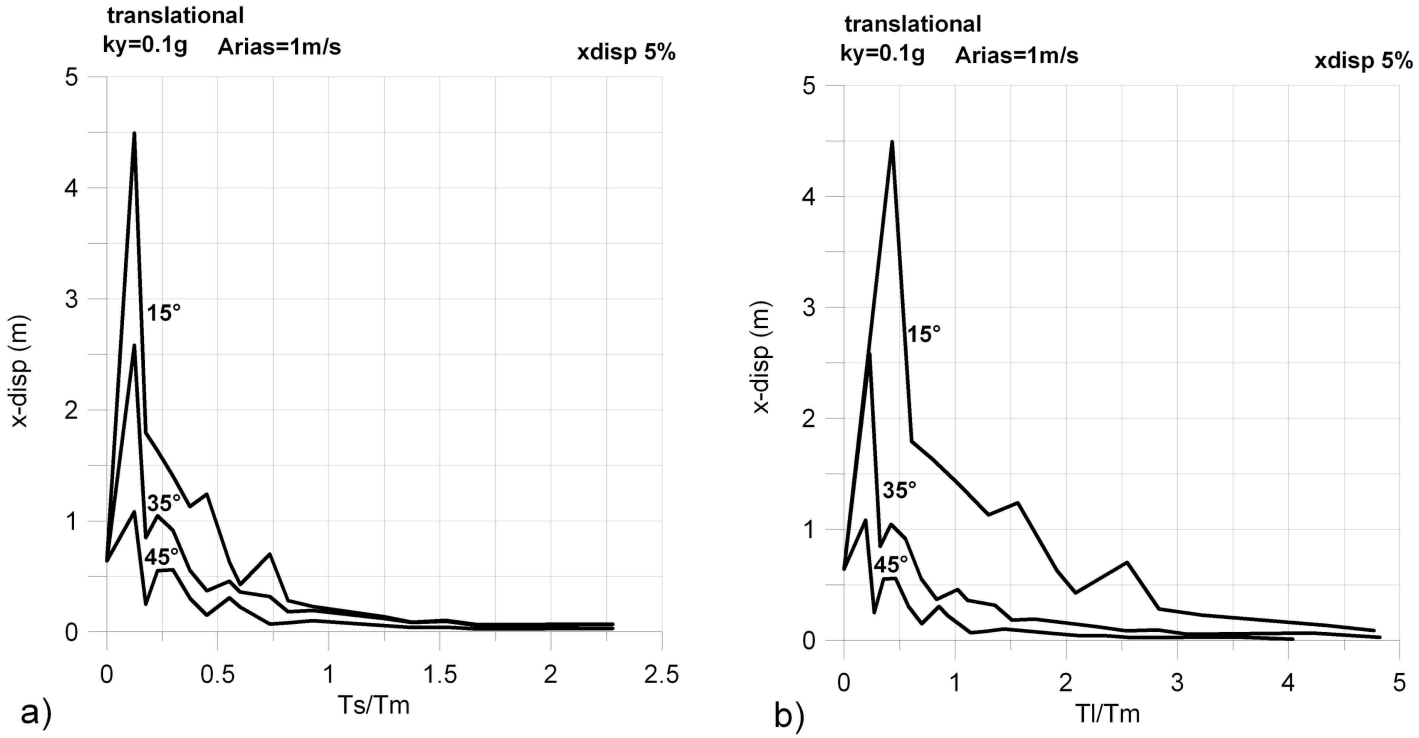

Fig. 8. Ts/Tm (a) and Tl/Tm (b) ratios obtained for the 15° slope configurations by applying 17 synthetic multifrequential dynamic inputs, characterized by an Arias intensity value close to 1 m/s.

CONCLUSIONS

The findings of the here discussed dynamic numerical modeling on step-like slope configurations hosting pre-existing landslide masses demonstrate the dependence of seismically-induced displacements on slope dip. This results are consistent with the higher seismic amplification functions A(f) which result at lower angles of dip (i.e. <35°). On the other hand, the effect of the frequency content of the seismic input on the resulting x-displacements of the existing landslide masses can be discussed in terms of characteristic ratios T_s/T_m and T_l/T_m ; the here presented preliminary study demonstrates the major role of 2D interactions between landslide mass and seismic inputs (i.e. the better correlation between T_l/T_m and x-displacements derived from dynamic numerical modeling with respect to the T_s/T_m ratio).
If compared with the classic sliding block approaches for computing co-seismic displacements (i.e. Newmark method as well as flexible block approaches) the here obtained results point out the significance of including the slope geometries (i.e. angle of dip of the slope) as well as the landslide mass dimension (i.e. T_l characteristic period) for providing more realistic values of seismically-induced displacements. In general this values can be overestimated, with respect to the ones computed by the sliding block approaches, depending on the Arias intensity of the seismic inputs, on the k_y of the landslide mass and on the Vs impedance contrast between the landslide mass and its substratum.

REFERENCES

Ashford, S.A., Sitar, N., Lysmer, J. and N. Deng [1997], "Topographic effects on the seismic response of steep slopes", Bul Seism Soc Am, 87, 701-709.

Athanasopoulos, G.A., Pelekis, P.C. and E.A. Leonidou [1999], "Effects of surface topography on seismic ground response in the Egion (Greece) 15 June 1995 earthquake", Soil Dynamics and Earthquake engineering, 18, 135-149.

Bakavoli, M.K., and E. Hagshenhas [2010] "Experimental and numerical study of topographic site effect on a hill near Tehran". Proc. *Fifth International Conference of Recent Advances in Geotechnical Earthquake Engineering and Soil Dynamics (May 24-29, S.Diego – California)*, 1-9.

Bird, J.F., and J.J. Bommer [2004], "Earthquake losses due to ground failure", Engineering Geology, 75:147-179.

Bouckovalas, G.D., and A.G. Papadimitriou [2005], "Numerical evaluation of slope topography effects on seismic ground motion", Soil Dynamics Earthquake Engineering, 25, 547-558.

Bozzano, F., Martino, S. and M. Priori [2006], "Natural and man-induced stress evolution of slopes: the Monte Mario hill in Rome", Environmental Geology, 50, 505-524.

Bozzano, F., Bretschneider, A., and S. Martino [2008°], "Stress-strain history from the geological evolution of the Orvieto and Radicofani cliff slopes (Italy)". Landslides 5(4), 351-366.

Bozzano, F., Lenti, L., Martino, S., Paciello, A., and G. Scarascia Mugnozza [2008b], "Self-excitation process due to local seismic amplification responsible for the reactivation of the Salcito landslide (Italy) on 31 October 2002", Journal of Geophysical Research, 113 , B10312, doi:10.1029/2007JB005309.

Bozzano, F., Lenti, L., Martino, S., Paciello, A., and G. Scarascia Mugnozza [2011], "Far-field seismic reactivation of large landslides due to self-excitation: new insights from the Cerda (Italy) case history", International Journal of Earth Sciences, 100, 861-879. DOI. 10.1007/s00531-010-0514-5.

Bray, J.D., and E.M. Rathje [1998], "Earthquake-induced displacements of solid-waste landfills", J. Geotech. and Geoenvir. Engrg., ASCE, 124(3), 242–253.

Danneels, G., Bourdeau, C., Torgoev, I., and H.B. Havenith [2008], "Geophysical investigation and dynamic modeling of unstable slopes: case-study of Kainama (Kyrgyzstan)", Geophysical Journal International, 175(1), 17–34.

Del Gaudio, V., and J. Wasowski [2007], "Directivity of slope dynamic response to seismic shaking", Geophys. Res. Lett, 34, L12301, doi:10.1029/2007GL029842.

Geli, L., Bard, P.Y, and B. Jullien [1988], "The effect of topography on earthquake ground motion: a review and new results", Bul Seism Soc Am, 78, 42-63.

Keefer, D.K. [1984], "Landslides caused by earthquakes", Geol Soc Am Bull, 95, 406-421.

Lenti, L., and S. Martino, S. [2010], "New procedure for deriving multifrequential dynamic equivalent signals (LEMA_DES): a test-study based on italian accelerometric records", Bulletin of Earthquake Engineering, 8, 813-846.

Lenti ,L., Martino, S., Paciello, A., Prestininzi, A., and R. Romeo [2011], "Insights into the ground motion records of the Honshu (Japan) earthquake of 11 March 2011", Italian Journal of Engineering Geology and Environment, 1(2011), 5-16.

Martino, S., and G. Scarascia Mugnozza [2005], "The role of the seismic trigger in the Calitri landslide (Italy): historical reconstruction and dynamic analysis", Soil Dynamics Earthquake Engineering, 25, 933-950.

Newmark, N.M. [1965], "Effects of earthquakes on dams and embankments", Geotechnique, 15(2), 139-159.

Nguyen, K.V. and B. Gatmiri [2007], "Evaluation of seismic ground motion induced by topographic irregularities". Soil Dynamics and Earthquake Engineering, 27, 183-188.

Papadimitriou, A.G. and Y. Chaloulos [2010], "Aggravation of the peak seismic acceleration in the vicinity of 2D hills, canyons and slopes", *Proc. Fifth International Conference of Recent Advances in Geotechnical Earthquake Engineering and Soil Dynamics (May 24-29, S.Diego – California)*, 1-12.

Rathje, E.M., and J.D. Bray [2000], "Nonlinear Coupled Seismic Sliding Analysis of Earth Structures". Journal of Geotechnical and Geoenvironmental Engineering, ASCE, 126(11), 1002-1014.

Rodriguez, C.E., Bommer, J.J. and R.J. Chandler [1999], "Earthquake-induced landslides: 1980-1997", Soil Dynamic Earthquake Engineering, 18, 325-346.

Sanchez-Sesma, F.J., and E. Rosenblueth [1979], "Ground motion at canyons of arbitrary shape under incident SH waves", Earthquake Engineering and Structural Dynamics, 7, 441-450.

Semblat, J.F., and A. Pecker [2009], "*Waves and vibrations in soils: earthquake, traffic, shocks, construction works*". IUSS Press - ISBN: 8861980309, pp. 499.

Sepulveda, S.A., Murphy, W., Jibson, R.W., and D.N. Petley [2005], "Seismically induced rock slope failures resulting from topographic amplification of strong ground motions: The case of Pacoima Canyon, California", Engineering Geology, 80, 336–348.

Zaslavsky, Y., and A. Shapira [2000], "Experimental study of topographic amplification using the Israel seismic network". Journal of Earthquake Engineering, 4(1), 43-65.

Zienkiewicz, O.P. [2005], "*The Finite Element Method*". McGraw-Hill (London), pp. 785.